Intelligent Approach for Segmenting CT Lung Images Using Fuzzy Logic with Bitplane

Z. Faizal Khan[†] and A. Kannan*

Abstract - In this article, we present a new grey scale image segmentation method based on Fuzzy logic and bitplane techniques which combines the bits of different bitplanes of a pixel inorder to increase the segmentation quality and to get a more reliable and accurate segmentation result. The proposed segmentation approach is conceptually different and explores a new strategy. Infact, our technique consists in combining many realizations of the image together inorder to increase the information quality and to get an optimal segmented image. For segmentation, we proceed in two steps. In the first step, we begin by identifying the bitplanes that represent the lungs clearly. For this purpose, the intensity value of a pixel is separated into bitplanes. In the second step, segmentation values are assigned for each bitplane based on membership table. The segmented values of foreground are combined and the segmentation values of background are combined. The algorithm is demonstrated through the medical computed tomography (CT) images. The segmentation accuracy of the proposed method is compared with two existing techniques. Satisfactory segmentation results have been obtained showing the effectiveness and superiority of the proposed method.

Keywords: Fuzzy logic, Bitplane method, Computed Tomography (CT), Segmentation, Unsupervised method.

1. Introduction

Image segmentation is one of the important tasks for image understanding and analysis. Segmentation partitions an image into a set of different regions. Each segmented object is homogeneous with respect to certain intensity characteristics like color and texture. The segmented objects in an image can be further separated from the background of the image. Most of the existing methods have used mostly thresholding concepts for segmentation. The different methods used for segmentation are statistical, geometrical and structural. Moreover, high-resolution X-Ray Computed Tomography (CT) is the standard for representing pulmonary images [10]. CT scans provide high spatio-temporal resolutions based on the hardware used for scanning. It also provides an outstanding contrast resolution for images pertaining to the pulmonary structure. Moreover, it has the capability to form a complete three-dimensional (3-D) volume [23, 25] of human thorax for a single breath. In the diagnosis of lung cancer, pulmonary CT-scanned images have been used for many applications including lung parenchyma analysis, density analysis and nodule detection. Lung segmentation is a precursor to most quantitative analysis [24].

Segmentation of medical imaging is useful for extracting information about the status of different tissues, different organs and other parts of the body [13]. The segmentation accuracy and higher decision confidence value of any lung analysis system for the identification of abnormalities rely mostly on an efficient lung segmentation technique. Hence the performance of segmentation based systems depends on the lung images [22]. In this paper, we propose a Fuzzy Logic based Bitplane [26] algorithm (FLBP) for the extraction of lungs from the background of a CT lung image. The extracted lungs are further used for identifying nodules and to perform further analysis.

The salient features of the proposed (FLBP) technique are:

a. It is an unsupervised method and is completely automatic.
b. No prior assumption is made about the type of features and type of contents, amount of noise and the contrast of the image.
c. The proposed method has a novel segmentation process based on assignment of 0 or 1 to pixels.
d. This method is robust in segmentation due to the incorporation of Fuzzy Logic with Bitplane.
e. The segmentation is accurate since it considers foreground and background of the image separately.

This FLBP method ensures that no excess pixel along the border of lungs is segmented. The remainder of the paper is organized as follows: Section 2 provides a survey of related works. Section 3 explains the proposed FLBP algorithm in detail by providing the details of each step.

---

†   Corresponding Author: Dept. of Computer Science and Engineering, College of Engg, Guindy, Anna University, India. (faizalkhan_111 @yahoo.co.in)
*   Dept. of Information Science and technology, College of Engg, Guindy, Anna University, India.

Section 4 depicts the results obtained from the work. Section 5 presents the conclusions on this work and suggests possible future works.

2. Related Works

Segmentation of lung in a high resolution CT (HRCT) image is performed using a pixel-based approach was proposed by Garnavi et al [1]. In their work, the decisions were based on crisp rules. Threshold based segmentation approach for segmenting lung region was proposed by Lin DT et al [7]. They have used a 5x5 median filter for removing the noise. The Foreground is separated by omitting the rim of the image along with the background. Samuel et al [4] have proposed a Rolling Ball-Algorithm for the segmentation of lung region from the CT lung image. They have applied the gray-level thresholding to obtain the lung regions. Moreover, they have segmented the lung region initially by removing the thorax from the background and then the lung region from thorax. Shiying et al [6] have developed an automatic method for segmenting lungs in CT lung images. They have divided their work into three main stages: (1) Gray-level thresholding to extract lung from CT-Scan image (2) Left and right lungs are separated through the identification of the anterior and posterior junctions by using dynamic programming and (3) smoothing of the irregular boundaries along the mediastinum, a sequence of morphological operations for acquiring results.

A combination of background-removal operator and iterative gray level thresholding was proposed by Antonelli et al [2]. In their work, the background was not eliminated well due to the presence of noise. Adaptive border marching algorithm was proposed by Jiantao Pu et al [9] which segments the lung region and reduces the under segmentation. They used the gray-level thresholding to obtain the lung regions and a flood-filling methodology to remove non-lung regions present after the thresholding. Ozekes et al [11] segmented the lungs of the CT images using Genetic Cellular Neural Networks (G-CNN). In their work, the lung regions were specified using the 8 directional searches and +1 or -1 value were assigned to each voxel. In the work proposed by Cao Leiet al [8], a rough image of lung was acquired by a combination of optimal thresholding and mathematical morphology. A self-fit segmentation algorithm was applied on the segmented result to obtain a refined output.

Manish Kakar [3] proposed a novel lung extraction algorithm by extracting the texture features using Gabor filter for filtering. In their algorithm, the features are combined to segment the lung region by using Fuzzy C Means clustering. Arfan Jaffar et al [5] proposed a combination of spatial Fuzzy C-Means and morphological techniques for segmenting the lung region from CT lung images. They have divided their work into three main stages namely Background removal, Preprocessing, and Morphological based operations.

Among them, a new histogram background removal operator has been used to remove the pixels around the lungs. Moreover, preprocessing is performed by smoothing and removing the noise present in the segmented image. Finally, morphological operations are used to separate the edges and to fill the small holes present in the segmented lungs. A joint serial image registration and segmentation methodology was proposed by Zhong Xue et al [16]. The major purpose of this algorithm is to segment a set of serial lung CT images. In their algorithm, the serial CT images are segmented based on the current deformations, and then the deformations among the serial images are iteratively refined based on the updated segmentation results. The main drawback of this technique is the presence of noise and discontinuities in the segmented lung region.

From the works found in the literature, it has been observed that most of the existing works used. Thresholding, Fuzzy C means, Neural networks and Background removal operators. However in case of medical applications, the accuracy provided by various phases of segmentation is not sufficient to make effective decisions. Therefore, it is necessary to propose a new and efficient technique to enhance the accuracy of segmentation.

3. Overview of the FLBP Method

In this paper, a fuzzy logic with bitplane method has been proposed for effective segmentation of lung images. This combination of fuzzy logic with bitplane method helps to make effective decisions under uncertainty. The FLBP method is a combination of bitplane processing of the image and fuzzy logic applied to each pixel. The FLBP method consists of the following steps:

a) The lung border values in the image are considered to decide the threshold value.
b) The gray scale lung image is separated into 8 monochrome images and hence the bit values from each bitplanes are obtained.
c) The 4 bits corresponding to the background of the intensity values are named as "lower nibble (LN)" and the other 4 bits corresponding to the foreground of the intensity values are considered as "upper Nibble (UN)".
d) Eight features are formed at each pixel. They are $v8$, $v7$, $v6$, $v5$, $v4$, $v3$, $v2$, $v1$. The numbers in the feature variables indicate the bitplane.
e) To assign a segmentation value of 1 or 0 to a pixel, a window of 3×3 pixels is considered. The 3×3 window is moved horizontally and vertically to cover the entire image.
f) Three signum membership functions are used to form a fuzzy membership value table in order to assign a

bit value 0 or 1to the bitplanes.

g) Inference is carried out for the foreground and background based on the bit values assigned using fuzzy membership table.

h) Defuzzification is performed with the maximum number 1 or 0 in a 3×3 windows considering foreground and background bit values of each pixel to decide the final segmentation.

i) Lung region is separated from the original image.

3.1 Description of proposed methodology

The FLBP system is based on bitplane processing. In this paper, the term bitplane is used to show the details of the image at various depths of information. Fuzzy rules are developed and used for determining the optimum segmentation of the lung from the background of a CT image. In this work, CT lung images are taken and represented using Hounds Unit (HU). Gray scale CT lung image is the normalization of the Hounds unit (HU) of the original CT image [12].

Table 1 shows the approximate representation of HU and gray scale. We have taken gray scale image as each pixel can be analyzed at bitplanes using the proposed FLBP method. A gray scale value of (63.25) representing the lung region was shown in the above table. The value can be 63.25 ± 40 to cover the entire area of lungs. The basic block diagram of the proposed system is given in Fig. 1.

Table 1. Representation of Hounds Unit and gray scale

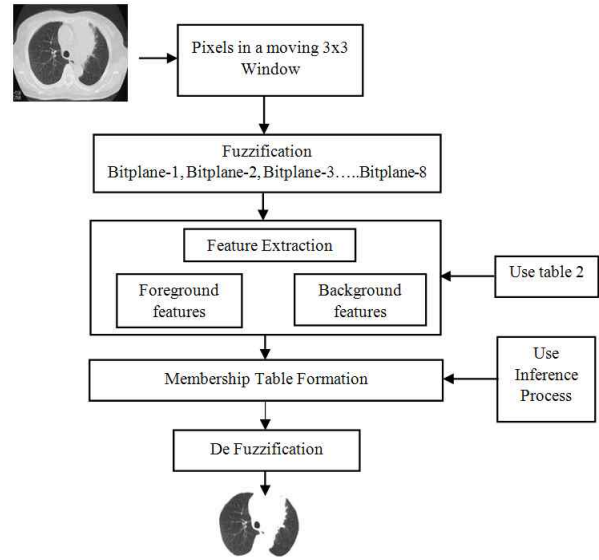| Unit	Air	Lung	Fat	Water	Soft Tissue	Muscle	Bone
Houns unit	-1000	-800	-94	0	39	40	101-1000
Gray scale	0	63.25	115	127	132	133	253

Fig. 1. Block diagram of FLBP system

3.1.1 Fuzzification of the Image

Fuzzification is the process of transforming the values from one crisp sets in to fuzzy set members for qualitative representation. In many Fuzzy segmentation methods like Fuzzy clustering, Fuzzy C-means and Fuzzy inference, transformation of intensity values to a different range of values is considered as an initial process. In this work, the transformation (Fuzzification) process is equivalent to the formation of 8 bitplanes and they are shown in Figs. 3(a-h). Each image contains 1or 0. Hence, each bitplane is a monochrome image. By observing each bitplane, the gradient of the boundary of lungs is calculated and a decision is made whether segmentation is required at such gradients. The degree of membership of each object in the image is computed on its association to each bitplane. The
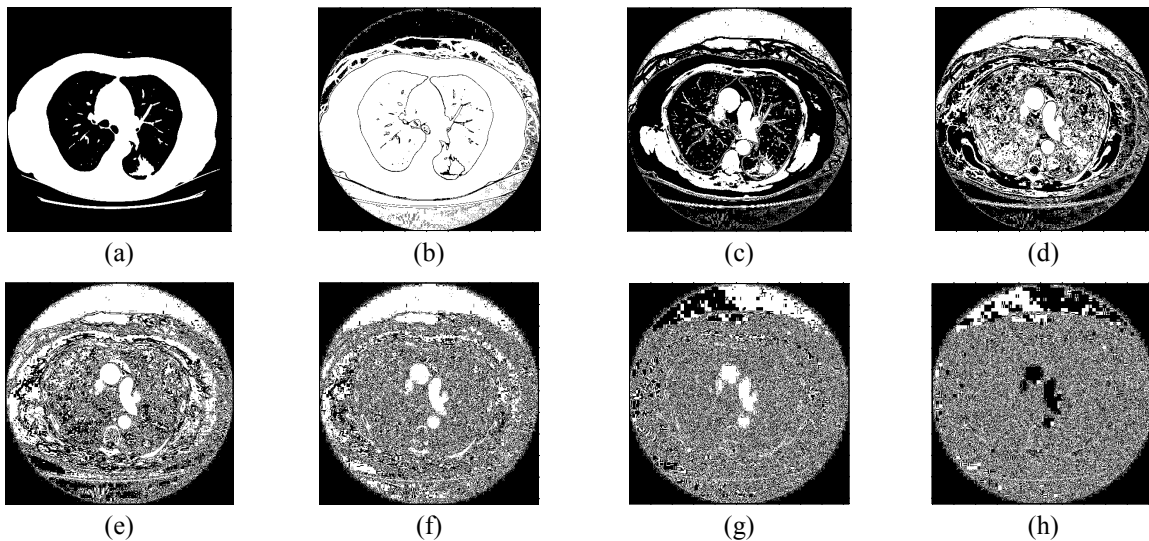

Fig. 2. Bitplane extraction results: (a) Bitplane-8; (b) Bitplane-7; (c) Bitplane-6; (d) Bitplane-5; (e) Bitplane-4; (f) Bitplane-3; (g) Bitplane-2; (h) Bitplane-1.

Table 2. Feature variables and its Calculation of feature values considering different bitplanes

Feature variable	Bitplane 8	Bitplane 7	Bitplane 6	Bitplane 5	Bitplane 4	Bitplane 3	Bitplane 2	Bitplane 1
V8	1 or 0	1 or 0	1 or 0	1 or 0	0	0	0	0
V7	0	1 or 0	1 or 0	1 or 0	0	0	0	0
V6	0	0	1 or 0	1 or 0	0	0	0	0
V5	0	0	0	1 or 0	0	0	0	0
V4	0	0	0	0	1 or 0	1 or 0	1 or 0	1 or 0
V3	0	0	0	0	0	1 or 0	1 or 0	1 or 0
V2	0	0	0	0	0	0	1 or 0	1 or 0
V1	0	0	0	0	0	0	0	1 or 0
	Upper Nibble				Lower Nibble			

histogram of each bitplane shows a degree of association of each object in a bitplane.

Fig. 2(a) presents the two lungs which are clearly visible from the background in bitplane 8. Profiles of the two lungs are clearly visible in Fig. 2(b) which is present in bitplane 7. The bitplane 6 represents the clearly visible center portion of the CT lung image. In Figs. 2(d-h), the lungs are not clear and the information appears to be noisy.

3.1.2 Feature Extraction

Feature extraction is a process of extracting representative values that will uniquely distinguish one image from a group of images. In this work, features extracted from lungs are different from the features of other parts of lungs. Many methodologies are available for extracting features of various objects in the lung image. These features are usually normalized values. The 8 features obtained at each pixel are grouped into two categories namely foreground and background features. Features (V8, V7, V6, V5) belongs to the background and features (V4, V3, V2, V1) belonging to the foreground. During the segmentation process, a 3x3 window of pixels are considered at a given instance. Hence, 8 features at each pixel and features of all the 9 pixels are considered to assign bit value either 1 or 0 at the center of 3x3 window.

Table 2 presents the feature variables and its possible bit values that can be present at different bit level. The first column of Table shows the feature variables. The subsequent columns represent monochrome values present at different bitplane of a pixel. Depending upon the gray scale value, the value of each bitplane can be 1 or 0. The foreground of the gray scale is in bitplanes (8 to 5). These bitplanes are named as Upper Nibble (UN). Similarly, the background of the gray scale is in bitplanes (4 to 1) is named as Lower Nibble (LN).

During the calculation of the foreground features, the lower bitplanes are replaced with 0 inorder to project the foreground of the image. Similarly, for the calculation of background features, the upper bitplanes are assigned with 0 inorder to project the foreground of the image. This can be noticed in Figs. 3(e-h) which show information in the background is not much useful for segmentation.

3.1.3 Membership Table Formation

Membership degree can be expressed by a mathematical function $\mu_A(x_1)$ that assigns each element in the set, a membership degree between 0 and 1. Let X is the universe of discourse and x_i is an element of X. A fuzzy set A in X can be defined as [14].

$$A = \{x_i, \mu_A(x_i) | x_i \epsilon X\} \tag{1}$$

The signum function [19] (Sig) is used for modelling the membership degrees. This degree of function is suitable for representing the white and black pixels. In this proposed work, we are focusing on segmentation by using bits. In such case, we get either 0 or 1rather than getting any intermediate outputs. Hence, we are choosing only signum function. Two breakages are required in the signum function in order to segment the UN and LN separately.

In this paper, we propose a new signum function called triple signum function that outputs the sign of a real number. This function outputs any one value from the three values (-1, 0, 1), when a real number is given as input to the proposed triple signum function. In order to propose this function, the existing signum function has been modified in this work for suiting our problem by outputting the bit values (1, 0) and hence the outputs of the signum function are (1, 0). This function can be also called as step function since only (1, 0) are obtained. Three signum functions are used in this work since three intervals levels of thresholds are used.

The width of signum function is controlled by two variables 'a' and 'b'. Similarly, the width of signum function 2 and 3 are controlled by 'c' which is present
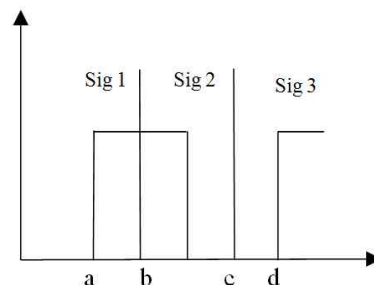

Fig. 3. Triple signum function

Table 3. Threshold value for foreground

Computed intensity value	Assigned segmentation value
>15 and <63	1
>100	1
≥ 63 and ≤ 100	0

Table 4. Threshold value for background

Computedintensity value	Assigned segmentation value
≤ 7	0
>7 and ≤ 15	1

between 'b' and 'd'. Depending upon the object to be detected, the location of 'c' can be changed.

This triple signum function as shown in Fig. 3 consists of three functions namely sig1, sig2, and sig3. Among them, sig1 and sig3 are the positive signum functions. As the values of the feature variables increase, the signum value changes from 0 to 1. Similarly in sig2, when the values of the feature variables increase the signum value changes from 1 to 0. Hence, sig2 is called as negative signum. For the UN bits, the sig2 and sig 3 are used.

The sig2 and sig3 function are suitable to represent the set of UN bits and is defined as

$$A = \mu_{A-sig(x)} = sig(x, a, b, c) \qquad (2)$$

$$= \begin{cases} 1 & b \leq x \leq c \\ 0 & c \leq x \leq d \\ 1 & x \leq d \end{cases} \qquad (3)$$

The sig1 and sig2 function is suitable to represent the set of LN bits and is defined as

$$A = \mu_{A-sig(x)} = sig(x, a, b) \qquad (4)$$

$$= \begin{cases} 0 & x \leq a \\ 1 & a < x \leq b \end{cases} \qquad (5)$$

The membership table is similar to a look up table and its formation is required to associate the input information in to output information. Membership table provided in Table 7 helps to assign the degree of membership value for the intensity values of different pixels.

3.1.4 Inference

The inference is a process of forming a new decision based on existing information. In this work, inference is carried out inorder to form the membership table by assigning output values based on feature values present in Table 6. At the end of inference, only two segmentation outputs are obtained at each pixel. The numbers in parenthesis in Table 7 are the bit values assigned based on the fuzzy rules shown below:

3.1.5 Defuzzification

Defuzzification is the process of combining the outputs of the inference for each pixel to a final segmented output

Fuzzy Rule 1	IF V8 $\geq \frac{2}{3}$ V7 then
	V8 = 1
	Else V8 = 0
	ENDIF
		Fuzzy Rule 5	IF V4 ≥ 5 then
			V4 = 1
			Else V4 = 0
			ENDIF

Fuzzy Rule 2	IF V7 $\geq \frac{2}{3}$ V6 then
	V7= 1
	Else V7 = 0
	ENDIF
		Fuzzy Rule 6	IF V3 ≥ 5 then
			V3 = 1
			Else V3 = 0
			ENDIF

Fuzzy rule 3	IF V6 $\geq \frac{2}{3}$ V5 then
	V6 = 1
	Else V6 = 0
	ENDIF
		Fuzzy Rule 7	IF V2 ≥ 2
			V2 = 1
			Else V2 = 0
			ENDIF

Fuzzy Rule 4	IF V5 ≥ 10 V5 = 1 Else V5 = 0 ENDIF	Fuzzy rule 8	IF V1 ≥ 1 V1 = 1 Else V1 = 0 ENDIF

that provides a segmented lung against the background of CT image. There are atleast 15 different defuzzification methods. Moreover, we have used "Maxima" defuzzification method [17]. Due to its generality, maxima refers to the total number of occurrence of either 1 or 0.The four steps used for defuzzification are as follows

Step 1 Assign one bit value for the foreground by combining bit values present in bitplane 8 till bitplane-5.

Step 2 Assign one bit value for background by combining bit values present in bitplane 4 till bitplane-1.

Step 3 Obtain only one bit values for each pixel based on the output of step 1 and 2.

Step 4 Obtain final segmentation values at the center of 3*3 window

Procedure Bit_assignment
Foreground (Table 8)
If
All the four bits in the UN==1**then**
   Assign '1' to the FG
else
Assign '0' to the FG.
end if
Background (Table 9)
if
$LN_{TN-one} >= 1$ **then**
   Assign 1 to BG
else
   Assign '0' to BG
end if.
Obtaining only one bit values(Table 10)
if
UN==1 and LN==1 **then**
Assign 1
else if
UN==1 and LN==0
Assign 1
else if

UN==0 and LN==0
Assign 0.
end if

Procedure Final_segmentation (Table 11)

if
Total number of 1 ≥ total number of 0 **then**
Center of the 3*3 window is 1
else
Center of the 3*3 window is 0
end if

The result obtained from final_segmentation procedure which was assigned to the 3*3 window is shown in Table 11. These values 0 and 1 help to get the final segmented lung region.

4. Experimental Evaluation

Segmentation accuracy has been evaluated in this work to assess the performance of proposed algorithm. In this section, we present the results of the proposed method qualitatively and quantitatively through image display and experiment measurements respectively. If the segmented object does not have any other smaller objects when compared to the same location of the original image, then it's easier to evaluate the segmentation accuracy based on counting the number of pixels in the original image.

4.1 Existing metrics to measure the segmentation accuracy

The Accuracy metrics A_s proposed by Zulaikha Beevi [18] is used to measure the accuracy of medical images. In our method, the segmentation accuracy A_s is computed using the formula.

$$A_{Pixel} = \frac{N_c}{T_p} * 100 \qquad (6)$$

where

A_{pixel} = segmentation accuracy
N_c = number of correctly segmented pixels in the lungs
T_p = total number of pixels corresponding to the lungs in the unsegmented image (Ground Truth)

Four grayscale CT images are considered for evaluating the quality of segmentation for our proposed method.

4.2 Proposed metrics to measure the segmentation accuracy

We have proposed another method to evaluate the segmentation accuracy by using the region properties of

Matlab. The important properties like solidity, perimeter and Area can be used.

The segmentation accuracy A_{prop} is computed using the following equation to evaluate the quality of the segmented lungs:

$$A_{prop} = \frac{S_{prop}}{O_{prop}} \times 100 \qquad (7)$$

$$S_{prop} = (Solidity + Area + Perimeter_{segmented}) \qquad (8)$$

$$O_{prop} = (Solidity + Area + Perimeter_{unsegmented}) \qquad (9)$$

where S_{prop} and O_{prop} are the region properties of the segmented and unsegmented images respectively.

Solidity is a scalar specifying the proportion of the pixels in the convex hull that are also in the region [15]. Area is the actual number of pixels in the region of interest. Convex Area is a Scalar that specifies the number of pixels in Convex Image. Convex Image is a Binary image (logical) that specifies the convex hull, with all pixels within the hull filled in.

The image is the size of the bounding box of the region. This property is supported only for 2-D input label matrices. Perimeter is the distance around the boundary of the region. Region props compute the perimeter by calculating the distance between each adjoining pair of pixels around the border of the region.

To prove the efficiency of the proposed segmentation algorithm, a sample 3x3 intensity values shown in Table 5 are taken from the border of the left lung from Fig. 4 (a) which are used in this paper to explain the segmentation process. The symbols p1, p2, 93, 94, 95, p6, p7, p8 and P9 indicate the pixel number.

Table 6 shows the computed total intensity values of features V8, V7, V6, V5 for the foreground and V4, V3, V2, V1 for the background based on the sample 3x3 intensity values. The intensity values assigned to each variables are based on the logic in Tables 3 and 4.

The features are grouped both as individual and combined. Individual features show the amount of contrast present in a bitplane and the combined features shows the amount of contrast present between the FG and BG of image. The contrast changes when different sets of combined features from the FG and BG are combined. When a large amount of contrast is present between FG and BG, then clear segmentation can be performed.

Fig. 4 shows the intensity values along the lung border for a 3*3 location. For both individual features and combined features, this graph reveals the possible level of intensity values present at a pixel both in the foreground

Table 5. Sample intensity values of 3 x 3 window

95(p1)	82(p2)	79(p3)
119(p4)	87(p5)	83(p6)
152(p7)	102(p8)	80(p9)

Table 6. Total intensity values calculation

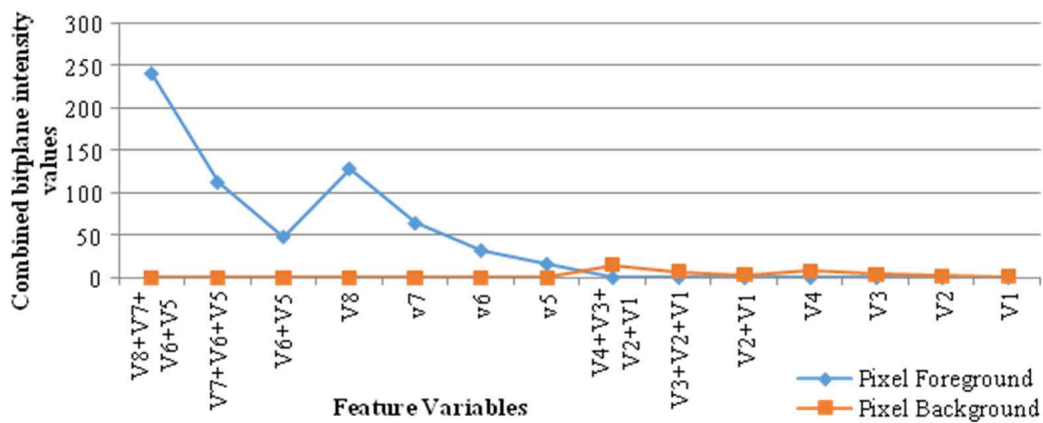| Variables in the upper nibble				Variables in the lower nibble						
				Combined Features			Individual Features			
				V4+V3+V2+V1	V3+V2+V1	V2+V1	V4	V3	V2	V1
		Total Intensity values	15	7	3	8	4	2	1
		Bit value assigned		1	1	0	1	0	0	0
Individual Features	V8+V7+V6+V5	240	1	1	1	0	1	0	0	0
	V7+V6+V5	112	1	1	1	0	1	0	0	0
	V6+V5	48	1	1	1	0	1	0	0	0
	V8	128	1	1	1	0	1	0	0	0
Combined Features	V7	64	0	0	0	0	0	0	0	0
	V6	32	1	1	1	0	1	0	0	0
	V5	16	1	1	1	0	1	0	0	0

Fig. 4. Feature value representation
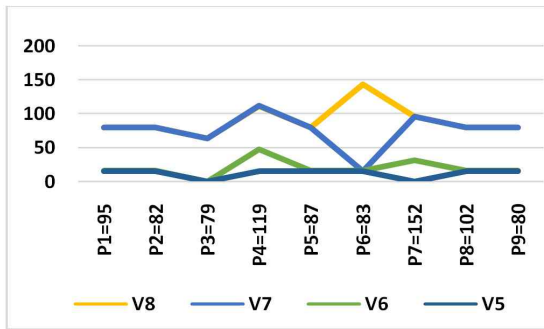
(a)
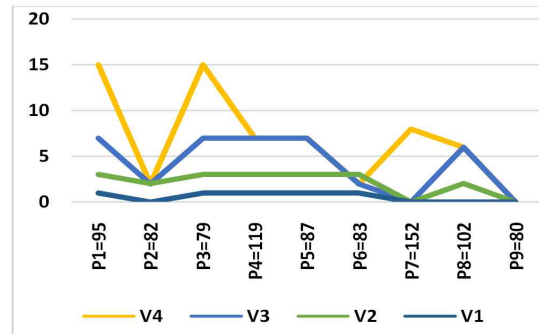
(b)

Fig. 5. Computed intensity values: (a) For foreground of 3x3 pixels; (b) for background of the 3x3 pixels

Table 7. Membership table for the 9 intensity values based on Fuzzy rules

	V8	V7	V6	V5	V4	V3	V2	V1
P1=95	80 (1)	80 (1)	16 (1)	16 (1)	15 (1)	7 (1)	3 (1)	1 (0)
P2=82	80 (1)	80 (1)	16 (1)	16 (1)	2 (0)	2 (0)	2 (1)	0 (0)
P3=79	64 (1)	64 (1)	0 (1)	0 (0)	15 (1)	7 (1)	3 (1)	1 (0)
P4=119	112 (1)	112 (1)	48 (1)	16 (1)	7 (1)	7 (1)	3 (1)	1 (0)
P5=87	80 (1)	80 (1)	16 (1)	16 (1)	7 (1)	7 (1)	3 (1)	1 (0)
P6=83	144 (1)	16 (1)	16 (1)	16 (1)	2 (0)	2 (0)	3 (1)	1 (0)
P7=152	96 (1)	96 (1)	32 (1)	0 (0)	8 (1)	0 (0)	0 (0)	0 (0)
P8=102	80 (1)	80 (1)	16 (1)	16 (1)	6 (1)	6 (1)	2 (1)	0 (0)
P9=80	80 (1)	80 (1)	16 (1)	16 (1)	0 (0)	0 (0)	0 (0)	0 (0)

Table 8. Bit values for UN

	C1	C2	C3
r1	P1(1)	P2(1)	P3(0)
r2	P4(1)	P5(1)	P6(1)
r3	P7(0)	P8(1)	P9(1)

Table 9. Bit values for LN

	C1	C2	C3
r1	P1(1)	P2(1)	P3(1)
r2	P4(1)	P5(1)	P6(1)
r3	P7(1)	P8(1)	P9(0)

and background. The intensity values present in the foreground is shown using Diamond and feature values present in the background is shown using Square. The plot shows that a significant slope with a difference of 60 degree in intensity values. Hence, segmentation value can be assigned at a grayscale of 100. This can be compared with the grayscale value mentioned for lung in Table 1.

The membership table is formed based on the fuzzy rules for the chosen block size of 3x3.through the inference process. The bit values assigned at each cell of the membership table is based on the product of bit values presented for UN and LN variables. The numbers in parenthesis in below table are the bit values assigned based on the fuzzy rules shown in the inference process

The Computed intensity values of foreground and background for the proposed method are shown in Figs. 5(a) and (b).

The above figure shows a computed intensity values for variables V8, V7, V6, V5, V4, V3, V2, and V1 respectively for all 9 pixels. From these graphs, it can be observed that the values "V6+V5" provides an optimum value for segmenting the foreground and "V4+V3+V2+V1" provides an optimum value for segmenting the background

The output bit values obtained from the procedure Bit_assignment for the foreground and background images are shown in Tables 8 and 9. Table 10 presents the output

Table 10. Obtained Bit values based on output of step 1 and 2

	C1	C2	C3
r1	P1(1)	P2(1)	P3(0)
r2	P4(1)	P5(1)	P6(1)
r3	P7(0)	P8(1)	P9(1)

Table 11. Final segmentation values

	C1	C2	C3
r1	P1(1)	P2(1)	P3(0)
r2	P4(1)	P5(1)	P6(1)
r3	P7(0)	P8(1)	P9(1)

Original CT image	Segmented result	Original CT image	Segmented result

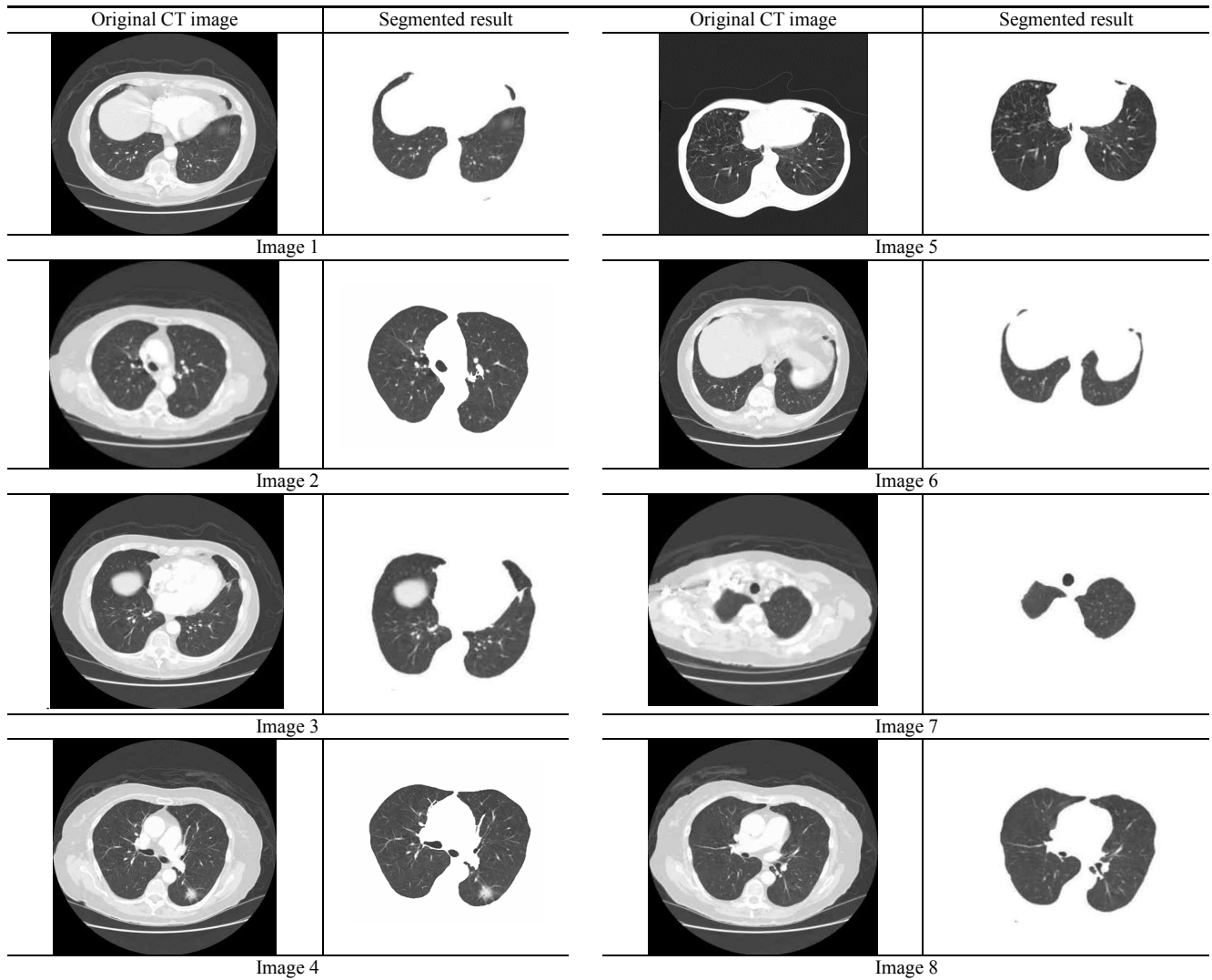Image 1   Image 5   Image 2   Image 6   Image 3   Image 7   Image 4   Image 8

Fig. 6. Results of the proposed system

Table 12. Number of pixels in segmented and ground truth images

Image	N_C	T_P (Ground truth)	A_{pixel} (%)
Image 1	40232	41882	96.06
Image 2	38002	38555	98.56
Image 3	31232	31896	97.85
Image 4	41362	42372	97.61
Image 5	32335	33438	96.70
Image 6	42878	43763	97.97
Image 7	36302	37406	97.04
Image 8	41862	42772	97.87

Obtained for only one bit values of each pixel based on the output of step 1 and 2. Table 11 depicts the final segmentation values at the center of 3x3 window. These values 0 and 1 help to get the final segmented lung region Fig. 9 shows the results obtained by applying the proposed FLBP technique on the test images. From this figure, it is evident that this FLBP technique produces much smoother results than the other schemes that have been used earlier. It can also be observed that almost all the existing techniques do not provide better results in which there are overlapping of intensities in lung parenchyma around chest wall. However, the FLBP technique has shown promising results on the different test cases which are shown in Fig. 9.

To enhance the efficiency of proposed segmentation algorithm, the performance measures based on statistical metrics have been computed and are given in Tables 12 and 13 for all the chosen lung images. The lung images for this experiment where chosen from a set of 300 images which are available in the LIDC database. The values shown in these table clearly indicates that there is a considerable improvement in the performance with respect to statistical method for the proposed algorithm over the lung image segmentation. Table 12 shows the total number of pixels present in the segmented and ground truth images.

Table 13 presents three region properties obtained by inbuilt command of Matlab software. The properties are solidity, area, and perimeter. These three values are obtained

for segmented and unsegmented images. The total of (Solidity+ Area+ Perimeter) of segmented image is divided by the total of (Solidity+Area+Perimeter) of unsegmented object. The segmentation accuracy calculated by Eq. (7) is as follows:

We proposed method 2 as an alternative to evaluate segmentation more meaningfully when compared to method-1. Ground truth image has been formed manually for all the four images using adobe photoshop. The percentage of segmentation is relative with respect to the ground truth image. The overall segmentation accuracy of 97.52 is obtained from the average value computed from the table.

4.3 Measurement and analysis of over/under segmentation

To evaluate the segmentation performance, we used two error metrics which are used to measure the over-segmentation and under-segmentation rates. We define over segmentation of the region of interest as the region volume that is regarded as tissue in this proposed segmentation method, and we also define the under-segmentation of the region of interest as the tissue that is regarded as region volume.

The over-segmentation and under-segmentation ratios for the 10 datasets are shown in Fig. 7. The average over-
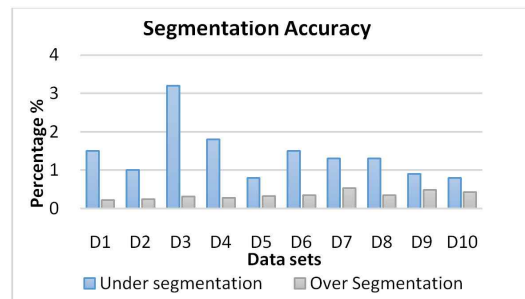

Fig. 7. Over segmentation/ under segmentation

Table 13. Segmentation accuracy of segmented and unsegmented images

Image	Region	Solidity	Area	Perimeter	Total	A_{prop}
Image 1	segmented	0.76535	43412	1541.4398	44954.156335	97.8112
	unsegmented	0.76535	44216	1743.4398	45960.156335	
Image 2	Segmented	0.679	37759	1832.9068	39592.5858	97.5557
	Unsegmented	0.679	38553	2030.9068	40584.5858	
Image 3	Segmented	0.71355	31096	1307.0235	32403.73705	97.2943
	Unsegmented	0.8376	31897	1407.0235	33304.8611	
Image 4	Segmented	0.8376	42361	1151.918	43213.81766	98.4958
	unsegmented	0.8376	42371	1501.918	43873.7556	
Image 5	Segmented	0.76605	32092	2411.0335	33303.73605	97.6043
	unsegmented	0.87008	33897	2407.0235	34304.8611	
Image 6	Segmented	1.6652	40759	2832.9568	43092.5358	97.7780
	unsegmented	0.679	38553	2030.9068	40584.5858	
Image 7	Segmented	1.649	48135	1651.918	45213.81766	98.8849
	unsegmented	1.6116	42371	2501.918	45873.7556	
Image 8	Segmented	1.6553	44412	2041.4398	46454.156335	96.4860
	unsegmented	1.6553	46216	1743.4398	49960.156335	

Table 14. Segmentation accuracy for different techniques

Segmentation accuracy	
Approaches	Segmentation (%)
Leader et al [20]	94.0%
Soleymanpour et al [21]	96.25%
Proposed Approach	97.52%

segmentation volume error per case is 0.34% of the entire volume, while the average under-segmentation is 1.41%.

4.4 Comparison of segmentation accuracy

Table 14 shows the detailed comparison of segmentation accuracy of the proposed method with two existing CT lung image segmentation techniques proposed by Leader et al [20], Soleymanpour et al [21]. From the table, it can be observed that the segmentation accuracy of the proposed methodology is higher when compared to the other existing methods for segmenting lung region form the Computed tomography lung images.

5. Conclusions and Future work

In this paper, a new fuzzy logic based bitplane thresholding method has been proposed for segmenting the medical images effectively. This method overcomes the limitations of existing methods where entire gray scale value of a pixel is considered. Fuzzy logic is used for each bit of a gray scale. Hence, more clarity is obtained in deciding the pixel which requires segmentation. To measure the performance of the proposed method, new metrics are proposed which measures the segmentation accuracy based on the number of pixels, properties and over/under segmentation ratios. The major contributions of this paper are improvement in segmentation accuracy and a new metrics for the effective measurement of segmentation accuracy. Future works in this direction can be the proposal of a new technique to analyze the presence of nodules in the segmented medical images.

References

[1] Garnavi R, Baraani-Dastjerdi A, Abrishami Moghaddam H, "A new segmentation method for lung HRCT images", *Proceedings of the Digital Imaging Computing: Techniques and Applications, IEEE*, pp. 52, 2005.

[2] Antonelli M, Lazzerini B, Marcelloni F "Segmentation and Reconstruction of the Lung Volume in CT Images". *20th annual ACM symposium on applied computing*, vol I. Santa Fe, New Mexico, pp. 255-259, March 2005.

[3] Manish Kakara Dag Rune Olsen, "Automatic Segmentation and Recognition of Lungs and Lesion fromCT Scans of Thorax", Comp Medical Imaging and Graphics. Vol. 33, pp. 72-82, 2009.

[4] Armato SG III, GigerML, Moran CJ, "Computerized detection of pulmonary nodules on CT scans. *Radio Graphics*", Vol. 19, pp. 1303-1311, 1999.

[5] M. ArfanJaffar, Ayyaz Hussain, Anwar Majid Mirza," Fuzzy Entropy Based Optimization of Clusters for the Segmentation of Lungs in CT Scanned Images", *Knowledge Information Systems*, Vol. 24, pp. 91-111, 2010.

[6] Hu S, Huffman EA, Reinhardt JM (2001) "Automatic Lung Segmentation for Accurate Quantification of Volumetric X-Ray CT Images", *IEEE Trans Medical Imaging*, Vol. 20, Issue-6, 2001.

[7] Lin DT, Yan CR, Chen WT, "Autonomous Detection of Pulmonary Nodules on CT Images with a Neural Network-Based Fuzzy system", *Comp Medical. Imaging and Graphics*, Vol. 29, pp. 447-458, 2005.

[8] Cao Lei Li Xiaojian Zhan Jie ChenWufan, "Automated Lung Segmentation Algorithm for CAD System of Thoracic CT", *Journal of Medical Colleges of PLA*, Volume 23, Issue 4, pp. 215-222, August 2008.

[9] JiantaoPu, Justus Roos, Chin A. Yi, Sandy Napel, Geoffrey D. Rubin, David S. Paik, "Adaptive Border Matching Algorithm: Automatic lung segmentation on chest CT images", *Comp Medical Imaging and Graphics* vol. 32, pp. 452-462, 2008.

[10] Wu M., Chang J., Chiang A.A., Lu J, Hsu H, "Use of quantitative CT to Predict Post-Operative Lung Function in Patients with Lung", *Journal of Cancer Radiology*" Vol. 191, pp.257-62, 1994.

[11] Ozekes S, Osman O, Ucan ON, "Nodule detection in a lung region that's segmented with using genetic cellular neural networks and 3D template matching with fuzzy rule based Thresholding", *Korean Journal of Radiology*, Vol. 9, pp. 1-9, 2008.

[12] Alan C Horwood, S J Hogan MA, P R Goddard, Jonathan Rossiter, "Image Normalization, a Basic Requirement for Computer-based Automatic Diagnostic Applications, pp. 1-26, May 2001.

[13] F Edward Boas & Dominik Fleischmann, "CT artifacts: Causes and reduction techniques" *Imaging Med*, Vol. 4, No. 2, pp. 229-240, 2012.

[14] Nuno Vieira Lopes, Pedro A. Mogadouro do Couto, Humberto Bustince, "Automatic Histogram Threshold Using Fuzzy Measures", *IEEE Transactions on Image Processing*, Vol. 19, No. 1, pp. 199-204, 2010.

[15] Hoffman EA, McLennan G, "Assessment of the pulmonary structure-function relationship and clinical outcomes measures Quantitative volumetric CT of the lung", *AcadRadiol*, Vol. 4, No. 11, pp. 758-776, 1997.

[16] ZhongXue, KelvinWong, Stephen T.C.Wong, "Joint registration and segmentation of serial lung CT images for image-guided lung cancer diagnosis and therapy", *Comp Medical Imaging and Graphics*, Vol.

34, pp. 55-60, 2010.

[17] Gunadi W. Nurcahyo, Siti Mariyam Shamsuddin, Rose Alinda Alias, Mohd. Noor Md. Sap, "Selection of Defuzzification Method to Obtain Crisp Value for Representing Uncertain Data in a Modified Sweep Algorithm", *JCS&T*, Vol.3, Issue 2, 2003.

[18] Zulaikha Beevi and Mohamed Sathik, "A Robust Segmentation Approach for Noisy Medical Images Using Fuzzy Clustering With Spatial Probability", *The The Int Arab J of Inf Tech*, Vol. 9, Issue. 1, 74-83, 2012

[19] A. K. Jain, Fundamentals of digital image processing, *Prentice-Hall*, New Jersey, 1989.

[20] Leader, JK, Zheng, B, Rogers, RM, Sciurba, FC, Perez, A, Chapman, BE, Patel, S, Fuhrman, CR & Gur, D, "Automated lung segmentation in X-ray computed tomography: Development and Evaluation of a Heu-ristic Threshold-based Scheme", *Academic Radiology*, vol. 10, no. 11, pp. 1224-36, 2003.

[21] Soleymanpour, E, Pourreza, HR, Ansaripour, E & Yazdi, MS, 'Fully Automatic Lung Segmentation and Rib Suppression Methods to Improve Nodule Detection in Chest Radiographs', *Journal of Med Signals and Sensors*, vol. 1, no. 3, pp.191-199, 2011.

[22] Jiahui Wang, James Dobbins, T & Qiang Li, "Automated Lung Segmentation in digital chest tomosynthesis", *Medical Physics*, vol. 39, no. 2, pp. 732-741, 2012.

[23] Meng, X, Qiang, Y, Zhu, S, Fuhrman, C, Siegfried, JM & Pu, J, "Illustration of the obstacles in computerized lung segmentation using examples", *Medical Physics*, vol. 39, no. 8, pp. 4984-4991, 2012.

[24] Guo Y, Zhou C, Chan HP, Chughtai A, Wei J, Hadjiiski LM, Kazerooni EA, "Automated iterative neutrosoaphic lung segmentation for image analysis in thoracic computed tomography", *Medical Physics*, Vol.40, issue.8, 2013.

[25] Sun S, Bauer C, Beichel R, "Automated 3-D segmentation of lungs with lung cancer in CT data using a novel robust active shape model approach", *IEEE Trans Med Imaging*, Vol. 31, No. 2, pp. 449-460, 2012.

[26] Gwanggil Jeon, "Watermarking on Bit Plane Arranged Images", *International Journal of Control and Automation*, vol. 6, no. 2, 2013.

Z. Faizal Khan received B.E degree in Computer Science and Engineering from Anna University, Chennai in 2008 and M.E. degree in Computer Science and Engineering from Anna University Tirunelveli in 2010. He is currently pursuing research in the area of medical image processing at Anna University, Chennai. His areas of interest include Medical image processing and Soft Computing.

A. Kannan Professor and Head, Department of Information Science and Technology, College of Engineering, Anna University, Chennai has 27 years' experience in teaching at Anna University, Chennai. His areas of research are Data Mining, Network Security, Database Management Systems, Artificial Intelligence, Software Engineering and Image Processing. He has published more than 85 research papers in reputed journals and conferences.